Journal of Alloys and Compounds, 203 (1994) 45–50
JALCOM 904

Partial phase diagram for the system $Cu_{0.5}Au_{0.5-x}Ni_x$ with $x \leqslant 0.15$

T. Shiraishi, M. Ohta and M. Nakagawa
Department of Dental Materials Engineering, Faculty of Dentistry, Kyushu University 61, Higashi-ku, Fukuoka 812 (Japan)
K. Fujii
Department of Dental Materials Science, Kagoshima University Dental School, Sakuragaoka, Kagoshima 890 (Japan)

(Received May 26, 1993)

Abstract

A partial phase diagram for the system $Cu_{0.5}Au_{0.5-x}Ni_x$ with $x \leqslant 0.15$ was determined by electrical resistivity measurements and X-ray powder diffraction. Substitution of only 2.8 at.% Ni for gold in equiatomic CuAu eliminated the CuAuII long-period superstructure from the phase equilibria. The presence of a two-phase coexistent region separating the CuAuI-type ordered phase and the disordered solid solution was evidenced. The solvus curve was determined by the parametric method and the solubility limits of nickel for the CuAuI-type superstructure at 300 and 320 °C were found to be 7.0 and 8.0 at.% Ni respectively.

1. Introduction

Gold–copper–nickel alloys are basic materials in jewellery [1]. Recently we reported that $Cu_{0.5}Au_{0.5-x}Ni_x$ alloys containing nickel up to about 12 at.% possess sufficient age hardenability for use as dental restorative alloys [2].

While an order–disorder transformation takes place in the gold–copper system [3] (Fig. 1), strong and weak phase separations occur in the gold–nickel [4] and copper–nickel [5] systems respectively. With regard to the ternary gold–copper–nickel system, Raynor [1] reviewed the experimental work on the phase diagram. Raub and Engel [6] determined boundaries of the solid state miscibility gap at temperatures from 300 to 950 °C and tie-lines in the two-phase region for isothermal sections at 400, 700 and 900 °C. According to their results, a solvus curve in the polythermal section $Cu_{0.5}Au_{0.5-x}Ni_x$ can be estimated to lie at 4.5 and 9.0 at.% Ni at 300 and 400 °C respectively. However, for the same polythermal section Kogachi [7] reported that a single phase with the CuAuI-type superstructure was stable up to a nickel concentration of 10 at.% below the order–disorder transformation temperature and that a nickel-rich disordered phase with the f.c.c. structure precipitated in ternary alloys with a nickel concentration of 12 at.% or more. Apparently there is a discrepancy between their results.

Furthermore, the partial phase diagram reported by Kogachi [7] indicates that no two-phase region separating the ordered CuAuI phase and the disordered solid solution (α) is present. However, Gantois [8, 9] and Faivre *et al.* [10] reported the presence of such a two-phase region in the system $Au_{0.5}Cu_{0.5-x}Ni_x$. Although the compositional section is different, it can be pointed out that there is a contradiction with respect to the (CuAuI + α) two-phase region.

Determination of the phase diagram is very important not only in designing the compositions of alloys but also in interpreting various properties of alloys of interest. In this research a partial phase diagram for the system $Cu_{0.5}Au_{0.5-x}Ni_x$ with nickel concentrations of up to 15 at.% was determined by electrical resistivity measurements and X-ray powder diffraction.

2. Experimental details

2.1. Sample preparation

Table 1 gives the chemical compositions of the alloys examined. Copper of 99.999% purity and gold and nickel of 99.99% purity were used as starting materials. Appropriate amounts of these component metals were melted together in a carbon crucible under an argon atmosphere and cast into a permanent mould. The ingots obtained were then subjected to alternate cold-rolling and homogenizing treatment at 840 °C. Plate samples 0.8 mm in thickness were prepared.

2.2. Electrical resistivity measurements

A thin plate sample of size $3 \times 20 \times 0.18$ mm^3, prepared from the previously mentioned plate sample, was

SSDI 0925-8388(93)00904-D

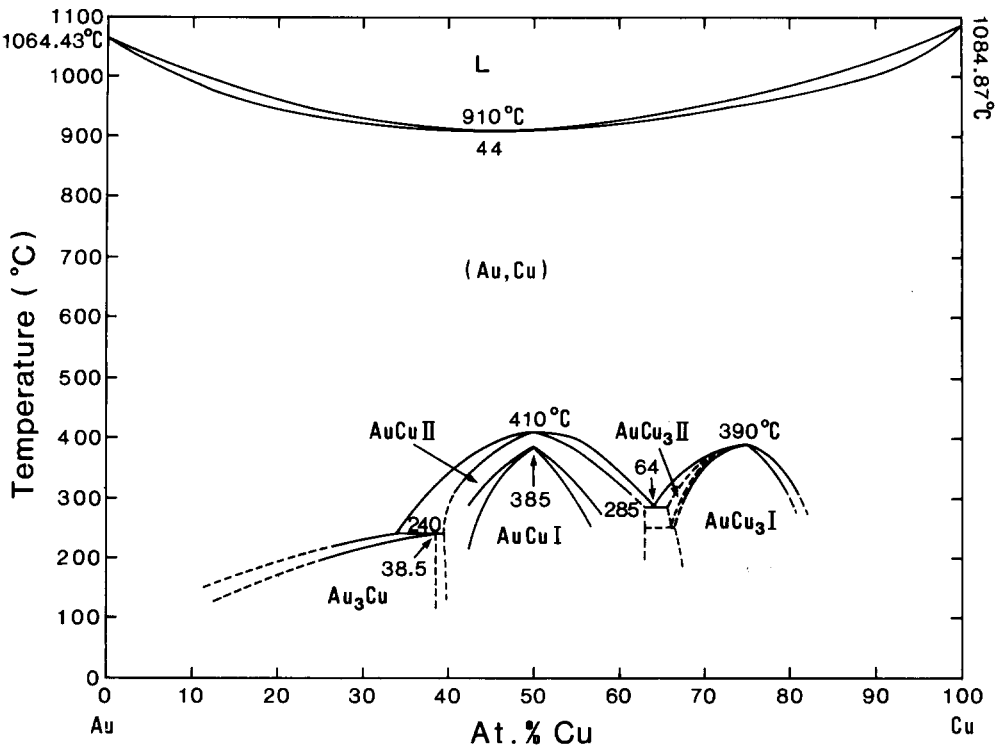

Fig. 1. The gold–copper phase diagram redrawn from ref. 3.

TABLE 1. Chemical compositions of alloys examined (analysed compositions)

Alloy	Element content (at.%)		
	Cu	Au	Ni
CA-1	49.9	50.1	0
CAN-2	50.0	47.2	2.8
CAN-3	49.9	44.1	6.0
CAN-4	49.9	41.0	9.1
CAN-5	49.9	38.2	11.9
CAN-6	50.0	35.0	15.0

solution treated at 700 °C for 30 min in a high purity argon gas stream and quenched into ice-brine. A couple of nickel wires 0.3 mm in diameter were then spot welded at both ends of the sample. Variations in electrical resistivity of the sample during continuous heating *in vacuo* were measured using the four-terminal potentiometric method with a direct current of 500 mA.

2.3. X-Ray diffraction

Powders that passed through a 330-mesh screen were produced using a rotating diamond disk. These powders were sealed in an evacuated silica capsule and subjected to the previously described solution treatment. They were then isothermally heated at the appropriate temperature for periods ranging from 20 000 to 50 000 min and quenched into ice-brine. The powders were examined in an RU-100PL standard-type diffractometer (Rigaku Co. Ltd., Tokyo, Japan). The X-ray source was a rotating anode copper target operating at 50 kV and 80 mA. Cu Kα radiation was used as the incident beam.

3. Results and discussion

3.1. Electrical resistivity–temperature curves

Figure 2 shows parts of the electrical resistivity *vs.* temperature curves for the alloys CA-1, CAN-2 and CAN-3 during continuous heating at a rate of 1.67×10^{-3} °C s^{-1}. The resistivity–temperature curves for each alloy have been shifted vertically from each other to avoid the overlapping of curves. For the alloy CA-1 two distinct inflection points were observed as indicated by the arrows "a" (around 385 °C) and "b" (around 410 °C). Referring to the gold–copper phase diagram [3] presented in Fig. 1, the temperatures of the inflection points "a" and "b" are thought to correspond to the CuAuI → CuAuII and CuAuII → disordered α phase transformation points respectively. However, in the electrical resistivity–temperature curves for the alloys CAN-2 and CAN-3 the inflection point reflecting the CuAuI → CuAuII phase transformation disappeared and temperature ranges within which the slope of the electrical resistivity–temperature curve was larger than that in the disordered α phase range appeared (between

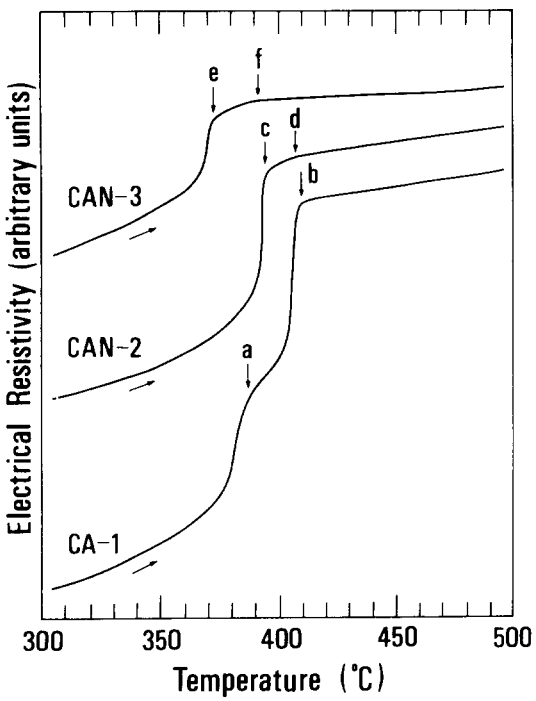

Fig. 2. Variation in electrical resistivity as a function of temperature for the alloys CA-1, CAN-2 and CAN-3.

the points "c" and "d" for the alloy CAN-2 and between the points "e" and "f" for the alloy CAN-3). Because the electrical resistivity of an alloy is sensitive to any structural change, these findings suggest that the partial substitution of nickel for gold in equiatomic CuAu eliminates the CuAuII long-period superstructure from the phase equilibria and that a (CuAuI + α) two-phase region may be produced. To confirm this hypothesis, we performed an X-ray diffraction study as presented in the following subsection.

3.2. Stable phases

Figure 3 shows an X-ray powder diffraction pattern of the alloy CAN-3 equilibrated at 380 °C for 20 000 min. This temperature is in the region between the points "e" and "f" in the electrical resistivity–temperature curves shown in Fig. 2. The subscripts "f" and "s" in the diffraction pattern indicate fundamental and superlattice reflections from the CuAuI-type ordered phase respectively. It was evidenced that the CuAuI-type ordered phase and the disordered α phase with the f.c.c. structure stably coexist at this temperature. Similar diffraction patterns were obtained for the alloy CAN-2 equilibrated at 400 °C, which is in the temperature region between the points "c" and "d" in Fig. 2, and the alloy CAN-4 equilibrated at 350 °C. These results made it clear that the (CuAuI + α) two-phase coexistent region was stably present in the system $Cu_{0.5}Au_{0.5-x}Ni_x$ with nickel concentrations up to about 9 at.%.

Figure 4 shows an X-ray powder diffraction pattern of the alloy CAN-5 equilibrated at 340 °C for 30 000 min, showing the three-phase coexistence of the CuAuI-type ordered phase and disordered α and nickel-rich α_2 phases. This finding reveals that the chemical composition of the alloy CAN-5 falls inside the solid state miscibility gap.

3.3. Determination of a solvus curve

The solvus curve in the system $Cu_{0.5}Au_{0.5-x}Ni_x$ was determined by the parametric method [11]. Powders of each alloy were equilibrated at the same temperature and quenched into ice-brine. The lattice parameters of the phases were measured by X-ray diffraction and plotted against the composition. Figure 5 shows the lattice parameters *vs.* composition curves for both the CuAuI-type ordered phase and the nickel-rich α_2 phase at the equilibrating temperature of 300 °C. At this temperature the single phase with the CuAuI-type superstructure was stable in the alloys CA-1, CAN-2 and CAN-3. On the other hand, a mixture of the CuAuI-type ordered phase and the nickel-rich α_2 phase with the f.c.c. structure was stable in the alloys CAN-4, CAN-5 and CAN-6. Therefore the lattice parameters a, c, c/a and $(a^2c)^{1/3}$ of the CuAuI-type ordered phase were plotted against the nickel concentration along with the parameter a of the α_2 phase. It was noted that the slope of each parameter–composition curve for the CuAuI-type ordered phase apparently changed at a nickel concentration of 7.0 at.%. This fact indicates that the solvus curve is correct for this composition at 300 °C.

The solubility limit of nickel for the CuAuI-type ordered phase at 320 °C and that for the α phase at 420 °C were found to be 8.0 and 11.2 at.% respectively. The resulting solvus curve is shown in the phase diagram (see Fig. 6).

3.4. Phase diagram

The resulting partial phase diagram for the system $Cu_{0.5}Au_{0.5-x}Ni_x$ is shown in Fig. 6. The substitution of only 2.8 at.% Ni for gold in equiatomic CuAu eliminated the CuAuII long-period superstructure from the phase equilibria. This result agrees well with that reported by Kogachi [7]. Sato and Toth [12], Gantois [8, 9, 13] and Faivre *et al.* [10] reported similar effects of nickel for the systems CuAu–Ni [12] and $Au_{0.5}Cu_{0.5-x}Ni_x$ [8–10, 13] respectively. It may not be easy to solve the problem of why the nickel addition to CuAu reduces the phase stability of the CuAuII long-period superstructure. However, considering the fact that the electron/atom ratio (e/a) of nickel is zero [12] and the previously reported experimental results that palladium (e/a = 0 [12, 14]) addition to CuAu also eliminated the CuAuII phase from the phase equilibria [12], the explanation by Sato

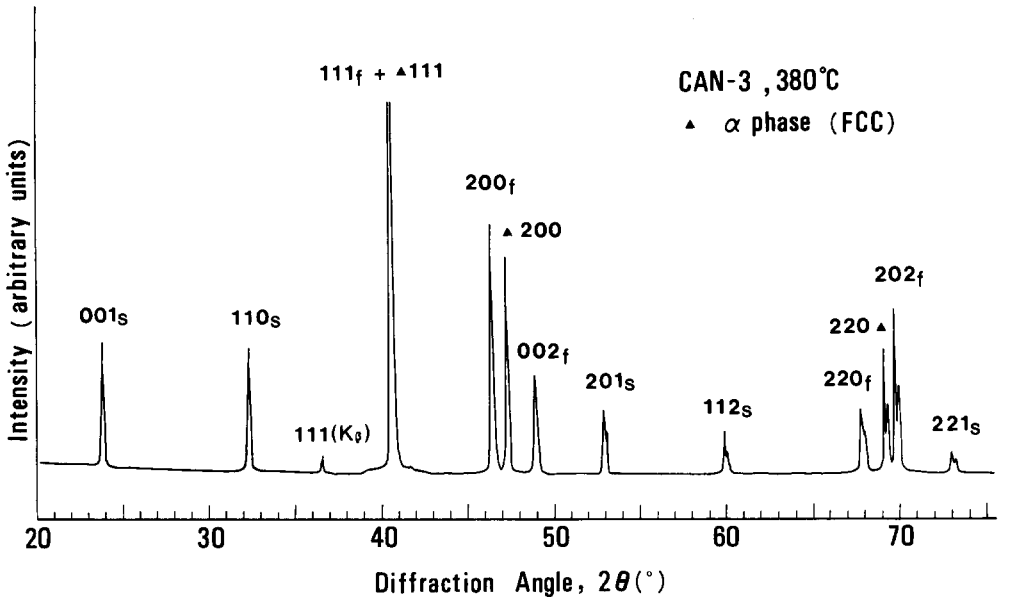

Fig. 3. X-Ray powder diffraction pattern of the alloy CAN-3 equilibrated at 380 °C for 20 000 min.

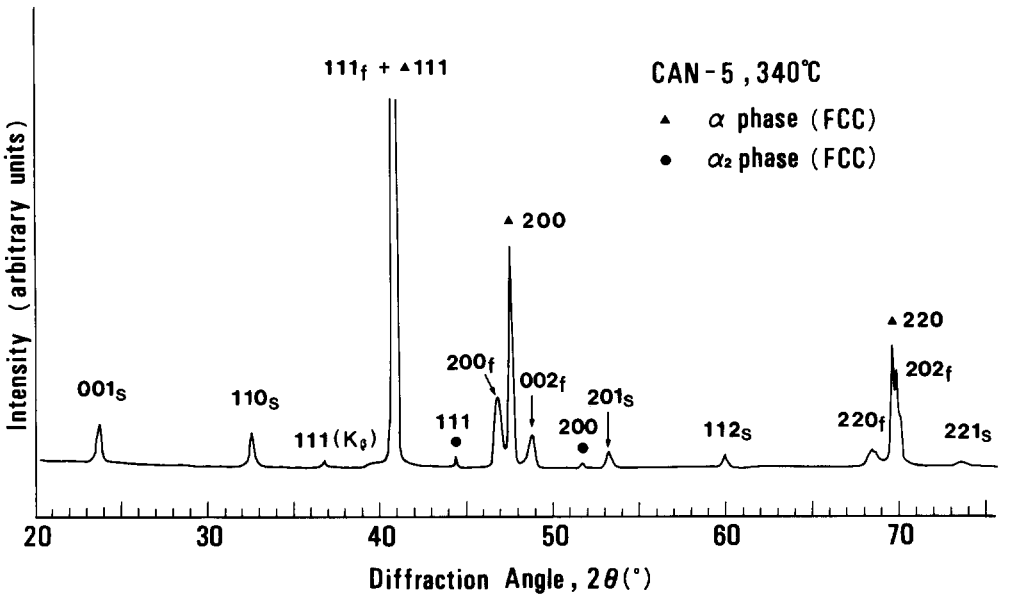

Fig. 4. X-Ray powder diffraction pattern of the alloy CAN-5 equilibrated at 340 °C for 30 000 min.

and Toth [12] that a reduction in the electron/atom ratio of an alloy reduces the phase stability of the CuAuII superstructure seems to be reasonable.

The presence of the two-phase coexistent region separating the ordered CuAuI phase and the disordered α solid solution was evidenced in the alloys containing less than about 9.5 at.% Ni. From the electrical resistivity–temperature curves shown in Fig. 2 the vertical width of this two-phase region was found to be about 13 °C at 2.8 at.% Ni and 20 °C at 6.0 at.% Ni. Although the presence of the (CuAuI + α) two-phase region has been shown in the system $Au_{0.5}Cu_{0.5-x}Ni_x$ [8–10, 13], it has not been reported in the system $Cu_{0.5}Au_{0.5-x}Ni_x$. This two-phase region changed into the (CuAuI + α + α_2) three-phase coexistent region in the alloys containing nickel in excess of the solubility limit, as shown in the phase diagram (Fig. 6).

Generally, it is well known that for alloys which undergo a first-order order–disorder transformation the ordered and disordered phases stably coexist near the stoichiometric composition under the condition of thermal equilibrium [15, 16]. Because the order–disorder transformation in Cu–Au alloys near the composition CuAu is known to be a first-order reaction [15, 16], the present evidence is well consistent with this general rule.

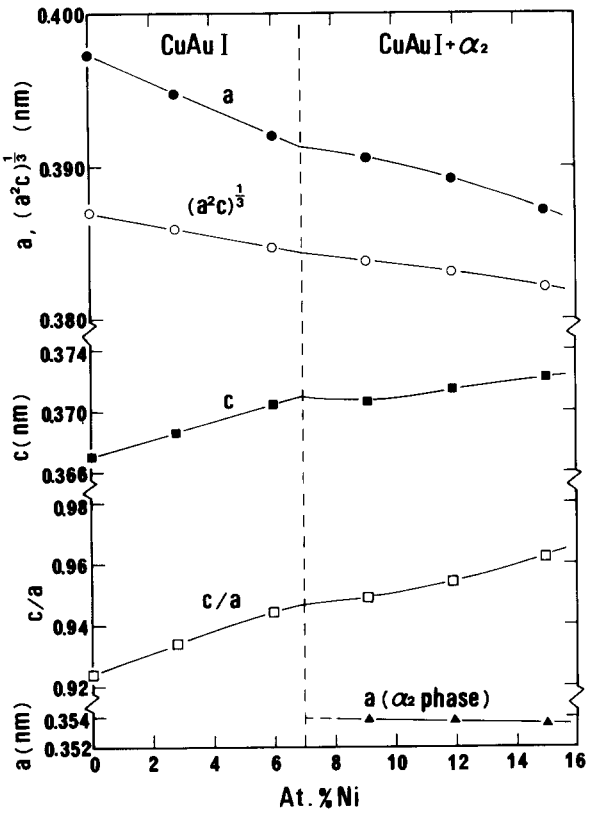

Fig. 5. Lattice parameters *vs.* composition curves for the CuAuI-type ordered phase and the nickel-rich α_2 phase at 300 °C.

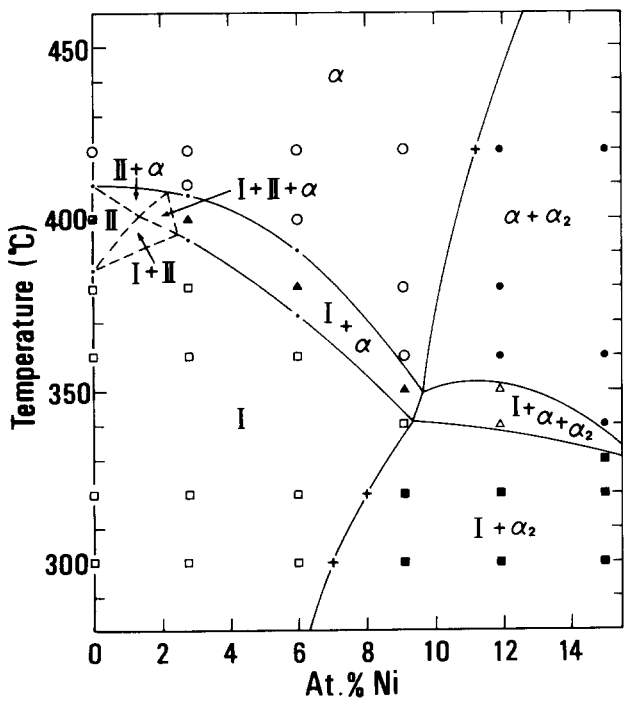

Fig. 6. Partial phase diagram for the system $Cu_{0.5}Au_{0.5-x}Ni_x$: ◪, CuAuII; □, CuAuI; ○, α; ▲, CuAuI+α; ■, CuAuI+α_2; ●, α+α_2; △, CuAuI+α+α_2.

It is seen that both the order and disorder temperatures fell with increasing nickel concentration. This trend agrees well with the previously reported partial phase diagram for the system $Au_{0.5}Cu_{0.5-x}Ni_x$ [8–10, 13].

4. Conclusions

A partial phase diagram for the system $Cu_{0.5}Au_{0.5-x}Ni_x$ with $x \leqslant 0.15$ was determined by electrical resistivity measurements and X-ray powder diffraction. The principal findings are as follows.

(1) The substitution of only 2.8 at.% Ni for gold in equiatomic CuAu eliminated the CuAuII long-period superstructure from the phase equilibria.

(2) The presence of a two-phase region separating the CuAuI-type ordered phase and the disordered α solid solution was evidenced in the alloys containing less than about 9.5 at.% Ni. The vertical width of the two-phase region was about 13 °C at 2.8 at.% Ni and 20 °C at 6.0 at.% Ni.

(3) The solubility limits of nickel for the CuAuI-type ordered phase at 300 and 320 °C were 7.0 and 8.0 at.% respectively. A nickel-rich α_2 phase with the f.c.c. structure precipitated in the $Cu_{0.5}Au_{0.5-x}Ni_x$ alloys containing nickel in excess of the solubility limit.

Acknowledgments

The authors thank Mrs. E. Yamamura for her line diagrams and the Ishifuku Metal Industry Co. Ltd. (Tokyo, Japan) for the preparation of sample alloys.

References

1 G.V. Raynor, in A. Prince, G.V. Raynor and D.S. Evans (eds.), *Phase Diagrams of Ternary Gold Alloys,* Institute of Metals, London, 1990, pp. 226–234.
2 T. Shiraishi, K. Fujii, M. Ohta and M. Nakagawa, *Mater. Charact., 30* (1993) 137.
3 H. Okamoto, D.J. Chakrabarti, D.E. Laughlin and T.B. Massalski, *Bull. Alloy Phase Diag., 8* (1987) 454.
4 T.B. Massalski, J.L. Murray, L.H. Bennett and H. Baker (eds.), *Binary Alloy Phase Diagrams,* Vol. 1, American Society for Metals, Metals Park, OH, 1986, pp. 288–290.
5 T.B. Massalski, J.L. Murray, L.H. Bennett and H. Baker (eds.), *Binary Alloy Phase Diagrams,* Vol. 1, American Society for Metals, Metals Park, OH, 1986, pp. 941–942.
6 E. Raub and A. Engel, *Z. Metall., 38* (1947) 11.
7 M. Kogachi, *Trans. Jpn. Inst. Met., 28* (1987) 102.
8 M. Gantois, *Mém. Sci. Rev. Mét., 65* (1968) 129.

9 M. Gantois, *J. Appl. Crystallogr., 1* (1968) 263.
10 R. Faivre, J. Hertz and M. Gantois, *Mater. Res. Bull., 3* (1968) 661.
11 B.D. Cullity, *Elements of X-Ray Diffraction*, Addison-Wesley, Reading, MA, 2nd edn., 1978, pp. 379–382.
12 H. Sato and R.S. Toth, *Phys. Rev., 124* (1961) 1833.
13 M. Gantois, *Compt. Rend., 257* (1963) 2104.
14 K. Ohshima and D. Watanabe, *Acta Crystallogr. A, 29* (1973) 520.
15 J.B. Newkirk, *J. Met., 5* (1953) 823.
16 Japan Institute of Metals (ed.), *Metals Handbook*, Maruzen, Tokyo, 4th edn., 1982, pp. 385–387.